

See discussions, stats, and author profiles for this publication at: <https://www.researchgate.net/publication/26784924>

Photoreactivity of a Push-Pull Merocyanine in Static Electric Fields: A Three-State Model of Isomerization Reactions Involving Conical Intersections

ARTICLE *in* THE JOURNAL OF PHYSICAL CHEMISTRY A · OCTOBER 2009

Impact Factor: 2.69 · DOI: 10.1021/jp904097k · Source: PubMed

CITATIONS

19

READS

18

4 AUTHORS, INCLUDING:



Anat Kahan

Hebrew University of Jerusalem

11 PUBLICATIONS 101 CITATIONS

[SEE PROFILE](#)



Shmuel Zilberg

Ariel University

66 PUBLICATIONS 1,123 CITATIONS

[SEE PROFILE](#)

Photoreactivity of a Push–Pull Merocyanine in Static Electric Fields: A Three-State Model of Isomerization Reactions Involving Conical Intersections

X. F. Xu, A. Kahan, S. Zilberg,* and Y. Haas*

Institute of Chemistry and the Farkas Center for Light Induced Processes, The Hebrew University of Jerusalem, Jerusalem, Israel

Received: May 3, 2009; Revised Manuscript Received: July 10, 2009

The photochemistry of a prototype push–pull merocyanine is discussed using a simple three-state model. As a derivative of butadiene, the model focuses on two isomerization reactions around the two double bonds of the butadiene backbone. As a molecule substituted by an electron donor and electron acceptor at opposite ends, its structure as well as its photochemistry are expected to be strongly affected by the environment. In polar solvents, a zwitterion transition state for each of the isomerization reactions is stabilized, and its energy is on the same order as that of the biradical one; this leads to the symmetry allowed crossing (S_0/S_1 conical intersection). It is shown that applying an external electric field or varying the solvent polarity changes the relative energies of the different transition states as well as that of the conical intersection, and thus different photochemical products can be obtained. In particular, the very existence of conical intersections is found to depend on these external parameters. This work provides a theoretical foundation for ideas expressed by Squillacote et al. (*J. Am. Chem. Soc.* **2004**, *126*, 1940) concerning the electrostatic control of photochemical reactions.

I. Introduction

Merocyanines are an interesting class of compounds because of their remarkable solvatochromic behavior,^{1–7} photochemical isomerization,^{8–14} and solvent-dependent hyperpolarizability.^{15–23} These molecules, which may be considered to be butadiene derivatives substituted by donor and acceptor groups at the opposite ends, are referred to as push–pull molecules. Their unique electronic structure is generally represented at the π level in terms of a resonance hybrid of two VB forms, quinonoid and zwitterion; the attractive properties of the merocyanines are traditionally understood in terms of these VB forms. Which of these structures dominates the ground state depends on the nature of the donor and acceptor positioned at the two opposite ends of the molecule and on the surrounding environments and leads to large changes in molecular properties. Applied electric fields as well as solvents have been found to affect the relative weights of the two VB structures in hybrid resonance of merocyanines in the ground state through polarization;¹⁵ this was demonstrated, for instance, in the case of Brooker's merocyanine (stilbazolium betaine).²⁴

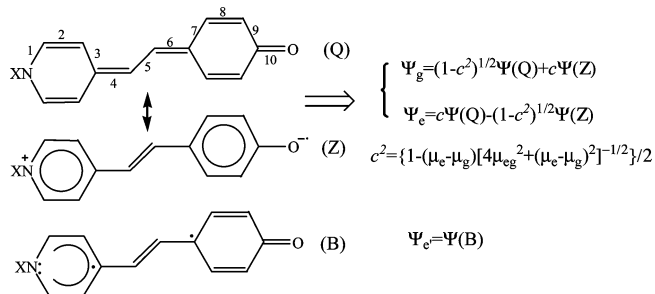
In this article, we are interested in the photochemical properties of these molecules and report our results on the prototype molecule I, in which the methyl group attached to the nitrogen atom in Brooker's merocyanine is substituted by a hydrogen atom. It is referred to as MRCN. Scheme 1 shows the two main VB forms of this molecule and a VB presentation of the ground state wave function Ψ_g , considered to be the in-phase combination of the two VB forms. The excited state (Ψ_e) conjugate to this state is formed by the out-of-phase combination of the same two VB forms. It is referred to as the twin state.²⁵ As suggested by ref 26, the relative contribution of the two forms may be derived from experimentally observable parameters using the following equation

$$c^2 = \frac{1}{2} \{1 - (\mu_e - \mu_g)[4\mu_{eg}^2 + (\mu_e - \mu_g)^2]^{-1/2}\} \quad (1)$$

where μ_g and μ_e are the dipole moments in the ground state and excited state, respectively, and μ_{eg} is the transition dipole moment between the two states. When $c^2 = 0.5$, the quinonoid and Zwitterion forms have equal weights in resonance hybrid; for $c^2 < 0.5$, the quinonoid form dominates the ground state; for $c^2 > 0.5$, the Zwitterion form dominates the ground state.

Squillacote²⁷ presented evidence of competition between two conical intersections through the electrostatic control of the

SCHEME 1: Quinonoid (Q), Zwitterion (Z), and Biradical (B) Structures for MRCN Showing the Notation Used to Name Bonds^a



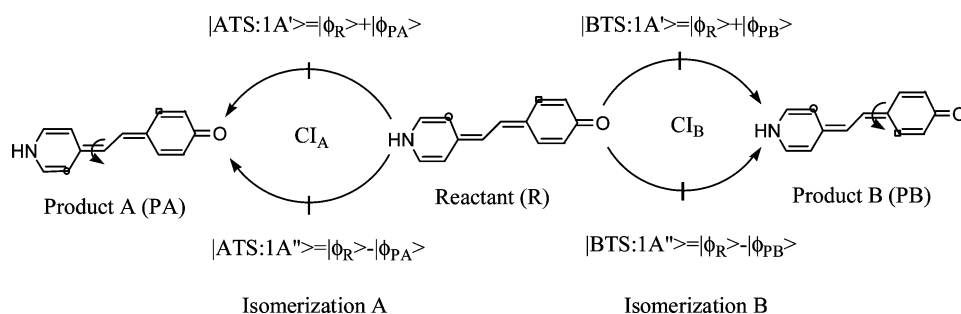
I. X=H MRCN

II. X=CH₃ Brooker's merocyanine

^a In the quinonoid form, bonds b4 and b6 are essentially double bonds, whereas in the zwitterion form, they are single. The in-phase and out-of-phase combinations of the Q and Z VB structures form the twin states: the ground state (Ψ_g) and one of the excited states (Ψ_e). The c^2 parameter quantifies the contributions of the Z form in the ground state: $c^2 = 0.5$ means the Q and Z forms have equal weights in resonance hybrid; for $c^2 < 0.5$, the Q form dominates the ground state; for $c^2 > 0.5$, the Z form dominates the ground state. Another excited state (Ψ_e') is a pure biradical state.

* Corresponding authors.

SCHEME 2: Two Possible Isomerization Products A and B Shown with the Two Longuet-Higgins Loops Pertaining to Them^a



^a Each loop passes through two different transition states (the zwitterion one denoted as TS:1A' and biradical one as TS:1A'') leading to the same product. The electronic wave functions of the transition states are expressed as the in-phase and out-of-phase combinations of the electronic wave functions of the reactant and product.

regioselectivity in the photoisomerization of the molecule with the butadiene fragment substituted by the donor/acceptor. Motivated by this work, we concentrate in this article on the two possible isomerization reactions around the two double bonds of MRCN. To the best of our knowledge, no high level ab initio calculation involving the configuration interaction was yet performed on a molecule of this size, with 16 electrons in 15 π orbitals. The existence of two VB structures for a substituted ethylene may lead, as shown elsewhere, to two different reaction pathways of the thermal cis-trans isomerization. One is via a biradical transition state (TS), the other is via a zwitterion TS.^{28–30} The presence of two transition states leading to the same product results in the existence of a conical intersection, which may be searched on the basis of the phase change theorem^{31–35} using elementary reaction coordinates. In the present case, there are two possible isomerization routes (Scheme 2) and therefore two possible conical intersections. Therefore, a two-legged phase inverting Longuet-Higgins loop³³ is constructed for each reaction, and one and only one conical intersection connecting the ground state (S_0) with the first excited state (S_1) can be located in the 2D domain for each loop. Therefore, under irradiation, the excited MRCN molecule can undergo two photoisomerization reactions, as shown in Scheme 2, and end up in either or both isomerization products A or B through the corresponding conical intersections.

In this theoretical study of MRCN, we discuss the photochemistry of the molecule in solvents of different polarities and also in the presence of a static electric field. In Section III.1, the effects of the solvent and the external electric field on the electronic and geometric structures of the molecular ground state are explored. An expected result has been obtained: increasing the field strength or the solvent polarity enhances the charge separation and leads to a geometric distortion from a quinonoid to a partially zwitterion-like structure. When the two low-lying $\pi \rightarrow \pi^*$ excited singlet states are considered in Section III.2, a three-state model (Scheme 1) is used to discuss the evolution of potential energy surfaces (PESs). As the electric field strength is increased, the energy gap between the twin states (the ground state Ψ_g and the excited state Ψ_e) initially decreases, followed by an increase. Another low-lying $\pi \rightarrow \pi^*$ excited singlet state ($\Psi_{e'}$) is of biradical nature irrespective of field effects, and the electric field has a small effect on its energy; therefore, a crossing between the two excited states may be observed as the field is varied. In Section III.3, we explore the photoisomerization channels of MRCN in the gas phase by searching for the S_0/S_1 conical intersection using the Longuet-Higgins loop strategy. Considering that various solvents or external electric fields are likely to reorder the energy levels of the ionic state

and biradical state, possible photoisomerization products and channels are also explored as a function of these parameters. The results suggest that by varying the environment or the electric field, the photoisomerization of MRCN may be controlled to yield different products.

II. Computational Details

The CASSCF³⁶ methodology implemented in the PCGAMESS³⁷ and MOLPRO³⁸ program suites has been used to study the interested stationary points (ground-state minima, transition states, excited states) of MRCN. The six higher-lying occupied π orbitals (out of eight) and the four lower virtual ones (out of seven), using all 12 π electrons, were included in the active space of the CASSCF calculations. (The orbitals are shown in Scheme S2 in the Supporting Information.)

The choice of the active space was made according to the size of molecule, $C_{13}NOH_{11}$, complex conjugated system (16 π electrons/15 π orbitals) and a strong donor–acceptor push–pull origin of this butadiene derivative. A different merocyanine–benzopyran was studied on the CAS level with 12e/11o active space.³⁹ The application of the CASSCF method to the spectroscopy of butadiene and other polyenes has been extensively discussed.^{40–44} For the unsubstituted molecule, Roos and others^{45,46} used CASSCF active space with both valence π orbitals and also more diffuse nonvalence π^* orbitals for the balanced representation of zwitterion and covalent structures. In contrast with the case of butadiene itself, the π^* excited states of merocyanine are found at a much lower energy than the Rydberg or σ^* states. Therefore, in distinction with butadiene, using only valence orbitals is adequate for the problem, even though as usual with CASSCF calculations, the excited state energies are somewhat overestimated compared with the experiment. In particular, as in the case of merocyanine, the molecule is nonsymmetrically substituted by the push–pull donor and acceptor pair, and the polar contribution is already large at the HF level. (The dipole moment of the merocyanine on the HF/cc-pVQZ level is ~13.0 D.) Therefore, the reference configuration includes the contribution of both polar and covalent components and the goal of CAS approximation is to reproduce this delicate balance. It is therefore assumed that this (12/10) CASSCF level of computation suffices for reproducing the nearly equivalent contributions of the polar versus the covalent forms and, consequently, the salient properties of the excited states.

In this work, two regions of the complete potential surface are considered. The Franck–Condon region is of interest for the light absorption stage and the processes immediately following it. For this region, a C_s symmetry constraint has been

imposed in all geometrical optimizations. This corresponds to an experimental situation in which the torsion motion is frozen, as realized, for instance, when the molecule is found in a solid cryogenic matrix. The other region is that of the transition states in which one of the double bonds is broken and one side of the molecule is rotated by $\pi/2$. No attempt was made to calculate the path leading from the FC region to the conical intersection. We located the two possible transition-state structures (zwitterion one denoted as TS:1A' and biradical one denoted as TS:1A'') of the double bond twisting by guessing a perpendicular structure of C_s symmetry with the same symmetric plane as that of the ground-state equilibrium geometry. As seen in Scheme 2, their electronic wave functions can be expressed as linear combinations (of A' or A'' symmetry in C_s) of the wave functions of the reactant and the desired product, respectively. Analytical frequency calculations have been performed using the GAMESS program.⁴⁷ Only one imaginary frequency responsible for the rotation around the double bond has been obtained for the optimized structures; their values are given in the Supporting Information. A complete list of all frequencies is available from the authors.

The first vertical excited states of the species with perpendicular geometry (two TS structures with different symmetry) have the opposite symmetry, respectively, as they are formed (at the given nuclear geometry) by the opposite combination.²⁸ Therefore, on the basis of the optimized geometry of the transition state, the energy of the state of different symmetry is calculated to figure out whether the optimized perpendicular structure is on the ground-state potential surface. If both optimized perpendicular species are found to be on the ground-state potential surface (i.e., both are transition states of ground-state reactions), then a conical intersection is sought along a coordinate connecting the two TS structures. The procedure for locating the conical intersection is based on a method developed by Dick.⁴⁸

In a separate set of calculations, a static electric field was added, and the corresponding changes in the structures and relative energies of a choice of stationary points were recalculated in the presence of external electric fields. The solvent effect is examined for two extreme cases: nonpolar solvents are represented by methylcyclohexane (MCH, $\epsilon = 2.0$), and strongly polar solvents are represented by acetonitrile (MeCN, $\epsilon = 37.5$). The solvents were modeled by the simple Onsager cavity model,⁴⁹ in which the cavity radius was used as a variable parameter. This might appear to be an oversimplified approximation for high-level CASSCF calculations. However, the goal of our study is the effect of an electric field; a simple experimental way to vary the field is by solvents of varying dielectric constants. Our use of typical solvents is only for “calibration”, approximately locating the field corresponding to a given solvent. For this purpose, the use of the simple lucid Onsager model with the cavity radius as a parameter appears to be adequate.

In addition, for comparison, the density functional method with the hybrid functional B3LYP^{50,51} also has been used to investigate the ground-state equilibrium structure of MRCN, in the gas phase and in solution, using Gaussian.⁵² The solvent effect was, in this case, estimated using the polarizable continuum model (PCM) model.⁵³

The cc-pVDZ basis set was used in all calculations.

III. Results and Discussion

III.1. Ground-State Minima of MRCN. **III.1.A. In the Gas Phase and in Solution.** The ground-state equilibrium geometries of MRCN, in the gas phase and in solvents with different

polarities (MCH: $\epsilon = 2.0$ and MeCN: $\epsilon = 37.5$), obtained at the CASSCF(12,10)/cc-pvdz level are displayed in Figure 1. The simple Onsager cavity model was used to estimate the solvent effect on the electronic and geometric structures of MRCN. Because the reaction field in this model is sensitive to the cavity's radius,⁵⁴ two different radius values (7.0 and 5.5 Å) were used to compare with experiment.⁵⁵ As Figure 1 shows, the molecule has a planar structure in all environments. This was verified by optimizing the structure without any symmetry constraints. The dipole moment at the ground-state minimum energy is calculated to be 10.80D in the gas phase, comparable to the experimental value ((10–15)D) for its analogs.^{56,57} As seen from Table 1, the calculated dipole moment of the ground state increases with the polarity of the solvent; the effect is more pronounced when the smaller radius (5.5 Å) is used.

To estimate the relative weights of the two VB structures in the resonance hybrid, we defined two geometric bond length alternation (BLA) parameters^{6,24} as the difference between the average length of “single” bonds and that of “double” bonds in the quinonoid form. (See Scheme 1 and Table 1 for their definition.) A large positive (negative) value of the BLA parameter means that the molecule can be represented to a very good approximation by a pure quinonoid (zwitterion) mesomeric structure. A vanishing BLA parameter indicates a cyanine-like structure with similar weights of the two forms.

The calculated BLA parameters, given in Table 1, indicate a clear predominance of the quinonoid structure in both gas-phase and nonpolar solvents. The present results are basically consistent with previous CS INDO studies⁶ on merocyanines. It should be noticed that when the polarity of solvents increases, the extent of bond length alternation decreases and the dipole moment of molecule increases; that is, the contribution of the zwitterion VB structure with large dipole moment increases in the more polar solvent.

III.1.B. Effect of External Electric Fields. When a polar molecule is subjected to an external electric field, the molecular charge distribution rearranges; this is revealed in the case of MRCN by a change in the relative weights of the two VB forms. The ground-state equilibrium geometries of MRCN were calculated in a static electric field in which the positive direction was from the oxygen atom to the nitrogen one, favoring charge transfer from the donor to the acceptor. The field strength was set between -0.0105 and 0.013 au ($1 \text{ au} = 5.142 \times 10^{11} \text{ V/m}$), and the corresponding BLA parameters were deduced to evaluate the relative weights of the two VB components. The field strengths employed are of the same order as the reaction fields determined for common polar liquids (10^7 – 10^8 V/cm).⁵⁸ The changes of the dipole moments of the molecule and BLA parameters as a function of field strength (ef) are displayed in Figures 2 and 3, respectively. At negative electric fields, some back charge transfer from the acceptor to donor occurs, resulting in a smaller dipole moment and larger BLA value compared with those in gas phase ($ef = 0$). At $ef = -0.0105$ au, the dipole moment along the field direction is reduced to zero, and the molecule assumes a pure quinonoid structure. Once a positive electric field is applied, the molecular dipole moment increases, whereas the BLA value is reduced. At an electric field near 0.0085 au, the $\text{BLA}(2) = [b_5 - (b_4 + b_6)/2]$ is lowered to be about zero, where the average value of the b_4 and b_6 bond lengths equals approximately the central bond b_5 . This indicates that at higher field strengths, the contribution of the zwitterion VB structure becomes more and more important and begins to be dominating. As the strength of the electric field rises to 0.012

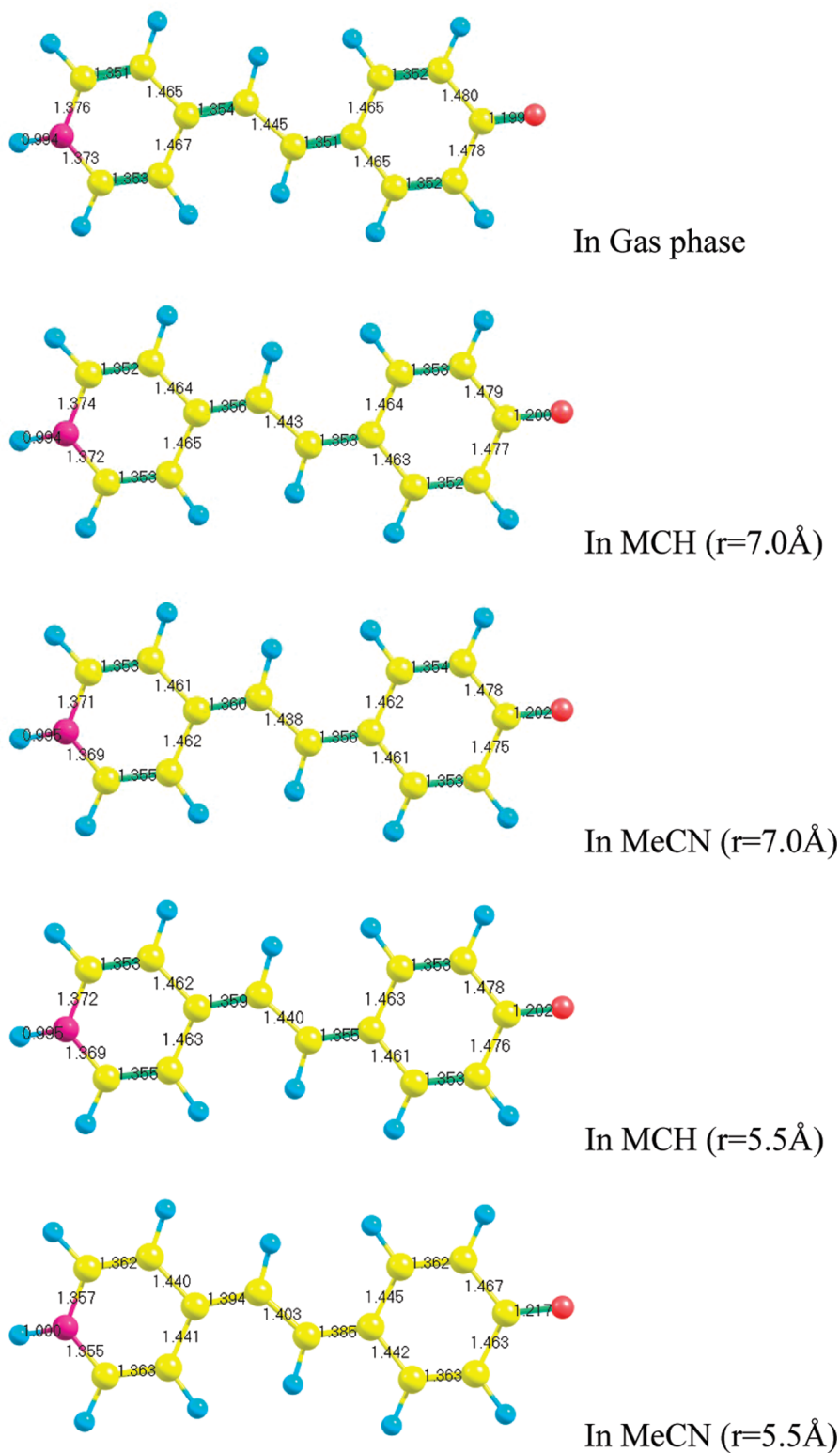


Figure 1. CASSCF-optimized equilibrium geometries of the ground state in different environments.

au, the dipole moment of MRCN increases to ~ 35 D and BLA(1) = $[(b_3 + b_5 + b_7 + b_9) - (b_2 + b_4 + b_6 + b_8)]/4$ reduces to 0.

Comparing the results in solvents and in the presence of electric fields shows that the effect of the nonpolar MCH ($r = 7.0 \text{ \AA}$) is similar to that of an electric field of 0.001 au, and the effect of MeCN ($r = 7.0 \text{ \AA}$) is similar to a field strength between 0.002 and 0.0035 au. When the smaller radius (5.5 \AA) is employed, the solvent effect is more pronounced: MCH ($r =$

5.5 \AA) behaves more like the electric field of 0.002 au, whereas for MeCN ($r = 5.5 \text{ \AA}$), the corresponding field is between ef = 0.007 and 0.0085 au. From the calculated BLA values in MeCN ($r = 5.5 \text{ \AA}$), the zwitterion and quinonoid VB structures are found to contribute almost equally to the resonance hybrid of the ground state.

III.1.C. DFT Results. As Table 1 shows, although the B3LYP-optimized equilibrium geometry of MRCN in the gas phase has a lower BLA value than that obtained at the CASSCF

TABLE 1: Calculated Dipole Moments (μ in debye) and BLA Parameters for the Optimized Ground-State Equilibrium Geometries in Different Environments^a

	CASSCF results		
	μ	BLA(1)	BLA(2)
in gas	10.80	0.112	0.093
in MCH ($\epsilon = 2.0$, $r = 7.0 \text{ \AA}$)	11.74	0.109	0.089
in MCH ($r = 5.5 \text{ \AA}$)	13.03	0.106	0.083
in MeCN ($\epsilon = 37.5$, $r = 7.0 \text{ \AA}$)	13.53	0.104	0.080
in MeCN ($r = 5.5 \text{ \AA}$)	23.05	0.063	0.014
DFT results			
	μ	BLA(1)	BLA(2)
in gas phase	14.37	0.070	0.020
in CH ($\epsilon = 2.0$)	18.56	0.060	0.005
in THF ($\epsilon = 7.6$)	25.68	0.043	-0.019
in MeCN ($\epsilon = 36.6$)	28.84	0.034	-0.032
in Water ($\epsilon = 78.4$)	28.03	0.032	-0.034

^a BLA(1) = [(b3 + b5 + b7 + b9) – (b2 + b4 + b6 + b8)]/4; BLA(2) = [b5 – (b4 + b6)/2]; See Scheme 1 for bond notation.

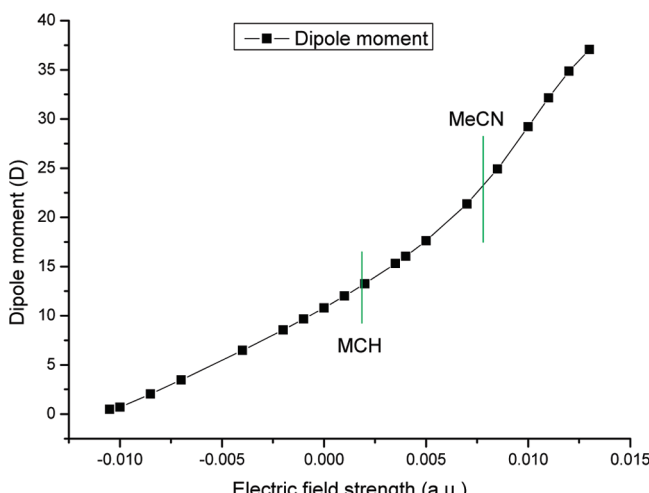


Figure 2. CASSCF calculated dipole moments of the MRCN ground state plotted against the electric field strength. For comparison, results obtained for the solvent effect using the Onsager model with a cavity radius of 5.5 Å are also shown.

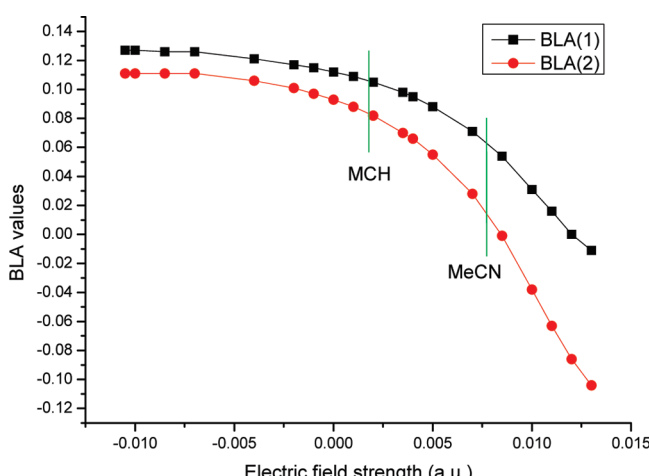


Figure 3. BLA parameters plotted against the electric field strength. For comparison, results obtained for the solvent effect using the Onsager model with a cavity radius of 5.5 Å are also shown.

level, the quinonoid VB structure is still the dominant one. Calculations at the B3LYP/PCM level suggest an obvious solvent effect on the geometrical and electronic structures of

TABLE 2: Vertical Transition Energies (kilocalories per mole) of the Low-Lying $\pi \rightarrow \pi^*$ States of MRCN^a

	2A'		3A'	
	ΔE	wave function ^b	ΔE	wave function ^b
gas	104.22	$\Psi_{e'}$ ($f = 0.29$)	112.55	Ψ_e ($f = 1.50$)
MCH ($r = 7.0 \text{ \AA}$)	103.57	$\Psi_{e'}$	108.32	Ψ_e
MeCN ($r = 7.0 \text{ \AA}$)	101.06	$\Psi_{e'}$	105.54	Ψ_e
MCH ($r = 5.5 \text{ \AA}$)	102.17	$\Psi_{e'}$	105.86	Ψ_e
MeCN ($r = 5.5 \text{ \AA}$)	96.71	Ψ_e	103.15	$\Psi_{e'}$

^a CASSCF/cc-pVQZ; ^b f : oscillator strength. Ψ_e : the wave function of the twin state; $\Psi_{e'}$: the wave function of the excited state of biradical nature.

MRCN, as shown in Table 1, similar to the CASSCF results with $r = 5.5 \text{ \AA}$, but different from those with $r = 7.0 \text{ \AA}$. In the nonpolar solvent, the two VB structures have similar weights. In the polar solvent, the zwitterion form becomes the more important one, leading to large dipole moment. Our DFT calculations agree with the B3LYP/6-31G** results of Ray.²²

Several additional solvents were included in the DFT calculations. The optimized structures in MeCN ($\epsilon = 36.6$) and water ($\epsilon = 78.4$), and the corresponding properties (dipole moment and BLA values) are basically the same, as shown in Table 1. This implies that the reaction field produced by MeCN represents a sufficiently strong polar environment, essentially leading to a complete transfer of one electron, and the molecule has a nearly pure zwitterion VB structure.

On the basis of the present results, when a larger radius (7.0 Å) of the cavity is used in the Onsager model, the CASSCF method will overestimate the contribution of the quinonoid structure in resonance hybrid in solvents, whereas the B3LYP/PCM model seems to overestimate the weight of the zwitterion form. The CASSCF results with the smaller radius (5.5 Å) appear to be reasonably satisfactory.

III.2. Two Lower-Lying $\pi \rightarrow \pi^*$ Excited States.

III.2.A. Franck–Condon Region: Vertical Transition Energy.

The strong absorption peak observed experimentally in the visible range has been assigned to excitation of the $\pi \rightarrow \pi^*$ transitions with large oscillator strength.^{1–3} Our calculated vertical excitation energies of the two lower-lying $\pi \rightarrow \pi^*$ singlet excited states in the Franck–Condon region using CASSCF are summarized in Table 2.

In the gas phase, the first vertical singlet $\pi \rightarrow \pi^*$ excited state (S_1 , 2A') has a relatively small dipole moment (cf. Figure 4) and is of biradical nature, principally represented by a superposition of the configurations ($\text{HOMO} \rightarrow \text{LUMO}_{+1}$) and the doubly excited one ($\text{HOMO} \rightarrow \text{LUMO}$)². The oscillator strength of the 1A'–2A' transition is much smaller than that of the next one (1A'–3A'). The latter corresponds to the strong HOMO \rightarrow LUMO electronic transition and the resulting state (3A') has a significantly larger dipole moment. The energy difference between the two $\pi \rightarrow \pi^*$ excited states is about 8 kcal/mol at the CASSCF level.

Similar to the calculations locating the ground-state minima, the solvent effect estimated with a large cavity radius (7.0 Å) is small. However, if a smaller radius (5.5 Å) is used, then the solvent effect on the energy levels of the two $\pi \rightarrow \pi^*$ excited states is significant. As Table 2 shows, in MCH, at the CASSCF level ($r = 5.5 \text{ \AA}$), the vertical transition energies of both of the two excited states (2A' and 3A') are reduced, whereas the energy of the 3A' state with large dipole moment shows an even larger decrease, resulting in a smaller energy gap (~3.7 kcal/mol) than that in the gas phase (8.0 kcal/mol). In the strongly polar MeCN,

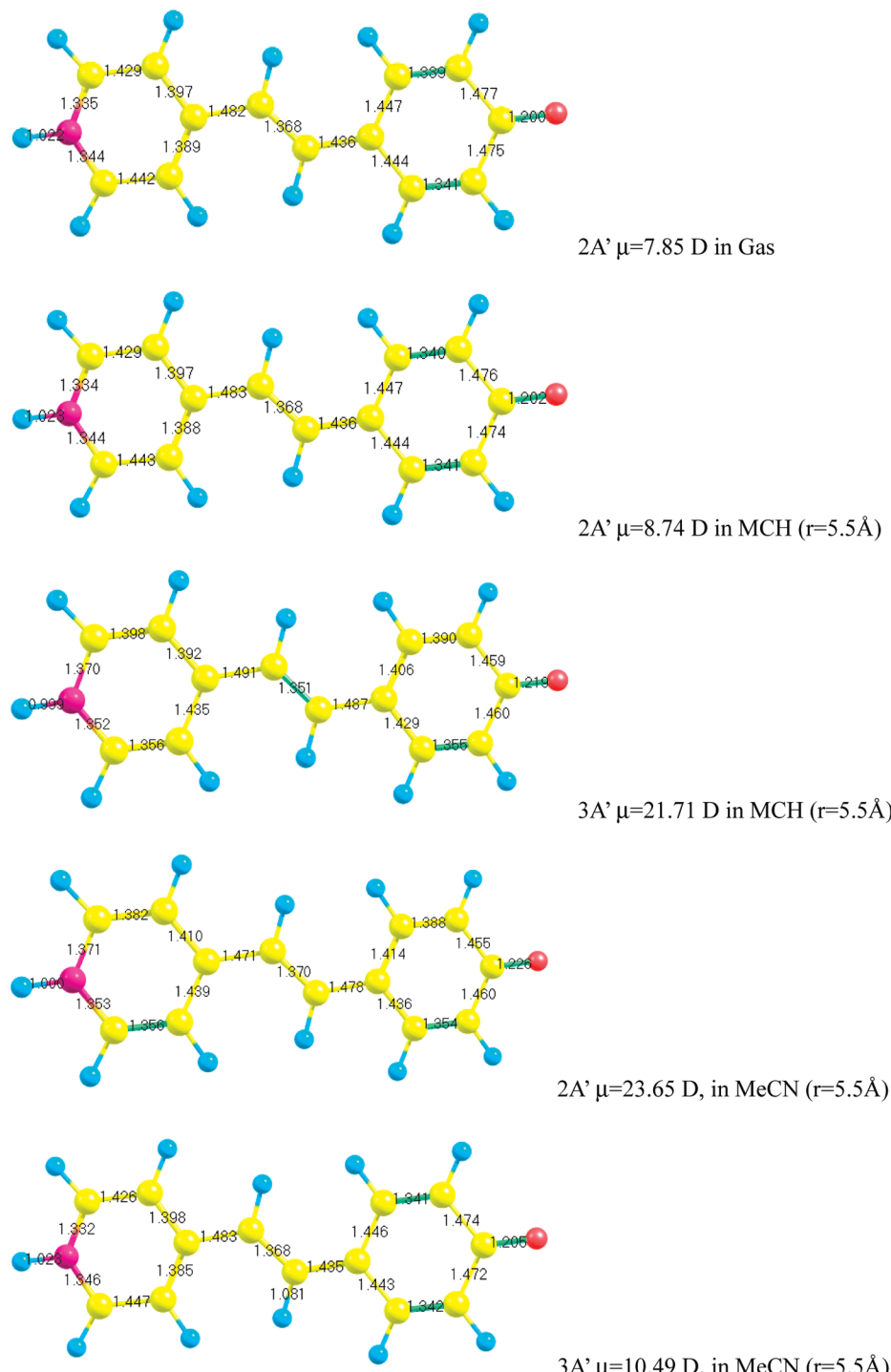


Figure 4. CASSCF-optimized equilibrium geometries and dipole moments of the two low-lying $\pi \rightarrow \pi^*$ excited states (2A' and 3A') in various environments.

an inversion of the two energy levels is obtained, and the vertical excitation energy of the biradical state with small dipole moment is slightly blue-shifted.

III.2.B. Optimized Structures of the Two Low-Lying $\pi \rightarrow \pi^*$ Excited States. The optimized geometries of the two low-lying $\pi \rightarrow \pi^*$ excited states (2A', 3A') have been investigated under C_s symmetry restriction at the CASSCF level, in the gas phase, and in solvents (with $r = 5.5 \text{ \AA}$).⁵⁹ As Figure 4 shows, the optimized structures of the excited states are significantly different from that of the ground state. In the excited states, the b4 and b6 bonds are longer for any environment, whereas, in contrast, the b5 bond shortens, becoming almost a double bond.

In the gas phase and in MCH, the optimized 2A' state is a biradical structure (Ψ_{e^-} in Scheme 1), with a smaller dipole moment than the ground state. Compared with the ground state, in the biradical 2A' state, only 0.1e in the gas phase (0.13e in MCH) is transferred back from the acceptor part (C_6OH_5^-) to the donor part (C_6NH_6^-). The optimized 3A' state in MCH, which exhibits zwitterion structure with a larger dipole moment (21.71D), is very close to the 2A' state, only 0.41 kcal/mol higher in energy. The larger zwitterion character of this state is consistent with its being the twin state of the ground state, formed by the out-of-phase combination of the quinonoid and zwitterion VB structures (Scheme 1). In the more polar MeCN,

TABLE 3: Some Calculated Properties of the Optimized Low-Lying Electronic States at the CASSCF Level^a

	charge population		μ	
	C ₆ NH ₆ —	C ₇ OH ₅ —	debye	BLA(2)
gas-1A'	0.119e	-0.12e	10.80	0.093
gas-2A'	0.02e	-0.019e	7.85	-0.091
MCH-1A'	0.158e	-0.158e	13.03	0.083
MCH-2A'	0.032e	-0.033e	8.74	-0.092
MCH-3A'	0.421e	-0.422e	21.71	-0.138
MeCN-1A'	0.361e	-0.365e	23.05	0.014
MeCN-2A'	0.441e	-0.44e	23.65	-0.105
MeCN-3A'	0.06e	-0.06e	10.49	-0.091

^a In the gas phase, the optimization for the twin state (3A') failed to converge, presumably as a result of the near degeneracy of the 2A' and 3A' states; the data in solution are obtained by the Onsager model with a cavity radius of 5.5 Å.

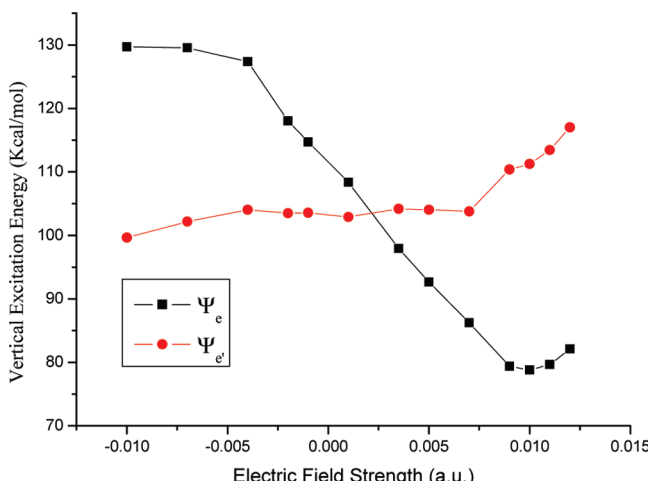


Figure 5. Plot of the calculated vertical excitation energies of the two low-lying $\pi \rightarrow \pi^*$ excited states as a function of the applied field strength. Ψ_e : the twin state; $\Psi_{e'}$: the biradical state.

the twin state is stabilized to be the 2A' state and is 10 kcal/mol lower in energy than the optimized biradical 3A' state.

As Table 3 shows, the BLA(2) value of the biradical excited state is the same in all environments. In contrast, the calculated BLA(2) absolute value of the excited state with larger dipole moment decreases in the more polar MeCN. This further supports our proposal that the excited state Ψ_e in Scheme 1 is the twin state of the ground state (Ψ_g in Scheme 1). In the polar MeCN, the contribution of the zwitterion VB structure in the ground state increases, and consequently, the weight of the zwitterion VB structure in the twin state (Ψ_e) is reduced; that is why the increment of the dipole moment is smaller for this state than for the ground state when the polarity of the solvent is increased.

III.2.C. Effect of Electric Fields on the Energies of the Two Low-Lying $\pi \rightarrow \pi^*$ Excited States. The vertical transition energies for the two low-lying $\pi \rightarrow \pi^*$ excited states as a function of electric field strength (in the range of -0.01 to 0.012 au) were calculated, and are shown in Figure 5.

As Figure 5 displays, a crossing of the two excited states occurs at $ef \approx 0.0021$ au. Under the influence of electric fields $ef < 0.0021$ au, the MRCN molecule behaves as a long-chain polyene;⁶⁰ the biradical excited singlet state ($\Psi_{e'}$) with small oscillator strength (corresponding to the dark 2A state of long-chain polyene) is below the twin state (Ψ_e) (corresponding to the bright ionic state 1B) at the Franck–Condon geometry. For field strengths larger than $ef = 0.0021$ au, the twin state (Ψ_e) is stabilized further and definitely becomes the first excited state.

In going from $ef = -0.01$ to 0.01 au, we calculate a decrease in the transition energy of the twin state (red shift), which can be ascribed to the fact that its dipole moment is basically larger than or nearly equal to that of the ground state. In the range of $ef = 0.0085$ to 0.01 au, the ground state can be described by nearly equal contributions from the two VB (quinonoid and zwitterion) structures, and the calculated c^2 parameter on the basis of eq 1 varies from 0.44 to 0.53. Therefore, in this range, the cyanine limit is reached, which is in agreement with the estimated BLA parameter. The blue shift in the transition energy of the twin state (Ψ_e) is observed from the point near $ef = 0.01$ au, where the zwitterion VB structure begins to dominate the ground state. The predicted electrochromic behavior of MRCN in varying electric field is consistent with that of donor–acceptor polyenes;⁵⁸ a red shift followed by a blue shift as a function of the applied field.

Because of small dipole moments difference ((~1–3)D) between the biradical state and the ground state at the Franck–Condon region, the vertical transition energy is less affected in the moderate fields of $ef = -0.004$ to 0.007 au, where the quinonoid form clearly dominates the ground state. In the presence of electric field $ef > 0.007$ au, the non-negligible contribution of the zwitterion VB structure in the resonance hybrid remarkably increases the dipole moment of the ground state, which stabilizes the ground state much more relative to the biradical state, leading to a blue shift in the transition energy of the biradical state, as shown in Figure 5.

III.3. Photoisomerization of MRCN. The calculations presented in Sections III.1 and III.2 indicate that the three mesomeric structures (quinonoid, zwitterion, and biradical) play an important role in the three low-lying electronic states of planar structures (the Franck–Condon region): the ground state (Ψ_g) and one excited state (Ψ_e) are twin states, respectively corresponding to the in-phase and out-of-phase combination of the quinonoid and zwitterion forms with strong coupling; the other excited state ($\Psi_{e'}$) is represented by a pure biradical structure. In the gas phase and in liquid solutions, after excitation to the FC region, the molecules will distort as the parent butadiene, and the system will cross over to the ground state. This process is most efficient when the S_1 and S_0 surfaces are close together, or even cross, as in a conical intersection (CI). We have not attempted to compute the trajectory leading from the FC region to the CI; rather, we focused on the effect that the solvent or electric field has on the region of the CI. It turns out that these parameters are strongly affecting that region, and in some cases, the degeneracy is found to be lifted. Because the energy and structure of the CI are closely related to those of the two transition states (Scheme 2), we begin the analysis by considering the effect of the environment on the transition states.

As noted in the Introduction, the isomerization around each of the two central double bonds (b4 and b6, Scheme 2) of MRCN could, in principle, proceed along two ground-state reaction coordinates, one with an ionic (zwitterion) transition state, which is of A' (C_s) symmetry (denoted as TS:1A'), and another one with a covalent (biradical) transition state, which is of A'' (C_s) symmetry (denoted as TS:1A''). At the perpendicular geometry, which is the structure of the two transition states for these isomerization reactions, the biradical and zwitterion species are the two lowest electronic states. Their relative energies do depend on the solvent's polarity or the field strength because of their different dipole moments. Under certain conditions, both the biradical and zwitterion TS structures can be located on the ground-state PES, implying that the isomer-

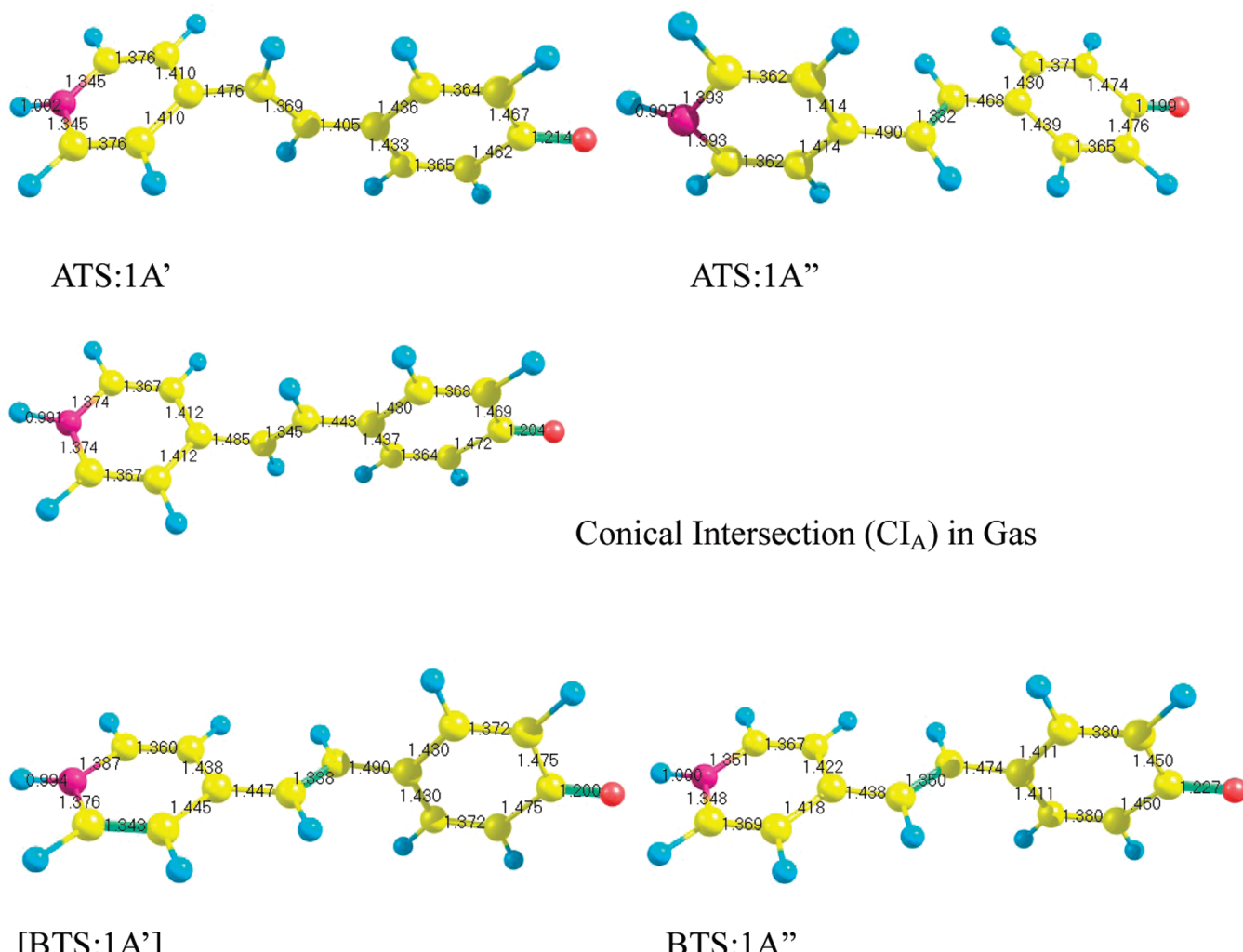


Figure 6. CASSCF geometries of transition states (TS:1A', TS:1A'') and conical intersection (CI) in the gas phase. Square brackets indicate that the optimized perpendicular structure is actually located on the excited-state PES. The letter “A” before “TS” represents the rotation around the b4 bond; the letter “B” is for the rotation around the b6 bond.

ization around the double bond can proceed indeed along two different ground-state reaction coordinates, and it is possible to locate the conical intersection using our “bottom-up” method²⁸ for the photoisomerization process of MRCN around b4 and b6 bonds. However, under different conditions, the lowest A' or A'' perpendicular structure may turn out to be on the excited state; this implies a single transition state and possibly the absence of a conical intersection.

III.3.A. Locating the Transition States and Conical Intersections. The transition states for isomerization around the b4 double bond are designated as ATS, and those for isomerization around the b6 double bond are designated as BTS. The transition states located in the gas phase at the CASSCF(12,10) level and their optimized geometries are shown in Figure 6.

For both isomerization modes, the geometries of the optimized TS structures are found to be very different from those of the ground-state equilibrium structure. In both, noticeable changes are obtained in the three central bonds (b4–b6): the b4 and b6 bonds are markedly lengthened, whereas b5 is shortened. Moreover, because of further charge transfer from the p orbital of nitrogen to the π^* orbital of C=O in the ionic transition state, both the N–H and the C–O bonds are weaker and longer. In the biradical TS structure (isomerization around the b4 bond), the nitrogen atom exhibits sp^3 hybridization.

As Table 4 and Figure 7 show, in the gas phase, the two TS structures (ATS:1A' and ATS:1A'') of the cis–trans isomerization around the b4 bond are almost isoenergetic on the basis of the CASSCF calculations. Using the method of ref 48 using PC-GAMESS, a 1A'/1A'' crossing has been located along the coordinate connecting the two TS structures, above the two transition states and below the first $\pi\pi^*$ state of FC region in energy. At this geometry, a state average calculation verified the existence of a S₁/S₀ conical intersection (CI_A), which is shown in Figure 6.

For the cis–trans isomerization around the second double bond (b6), only the biradical species (BTS:1A'') was found to be a transition state. The lowest-lying ionic perpendicular structure ([BTS:1A']) (analogous to the ionic transition state ATS:1A') has in fact been located, but it was found to lie on the excited-state potential surface. It is thus not a transition state on the ground-state PES; a lower-lying biradical structure exists on the ground state at the same geometry. Square brackets ([]) are used to mark the distinction, whereas the notation TS is preserved because under different conditions, this species may become a ground-state entity and a real transition state on the ground-state PES.

Following a reviewer's suggestion, we have recalculated the structure of the first conical intersection in the gas phase, CI_A,

TABLE 4: Relative Energies (kilocalories per mole) and Dipole Moments (μ , in debye) of the Optimized Transition States in Gas Phase and in Solvents^a

		rotation around the b4 bond		rotation around the b6 bond	
		$\Delta E(\text{CASSCF})^b$	μ^c	$\Delta E(\text{CASSCF})^b$	μ^c
gas	TS:1A'	47.05	26.80	[54.82]	30.16
	TS:1A''	49.76	6.39	41.42	8.70
MCH ($r = 7.0 \text{ \AA}$)	TS:1A'	41.56	29.11	[47.66]	32.40
	TS:1A''	[50.42]	6.80	47.50	8.37
MCH ($r = 5.5 \text{ \AA}$)	TS:1A'	34.58	32.14	38.94	34.92
	TS:1A''	[51.35]	7.17	49.42	8.85
MeCN ($r = 7.0 \text{ \AA}$)	TS:1A'	32.03	33.23	35.88	35.75
	TS:1A''	[51.70]	7.30	[42.89]	9.01
MeCN ($r = 5.5 \text{ \AA}$)	TS:1A'	7.82	41.66	9.17	42.56
	TS:1A''	[56.41]	8.44	[46.89]	10.52

^a Square brackets indicate that the structure lies on S₁. ^b Relative to the corresponding ground-state minimum. ^c Ionic transition state at perpendicular geometry almost corresponds to a complete intramolecular charge transfer; the large calculated dipole moment may indicate the possible limit of the model.

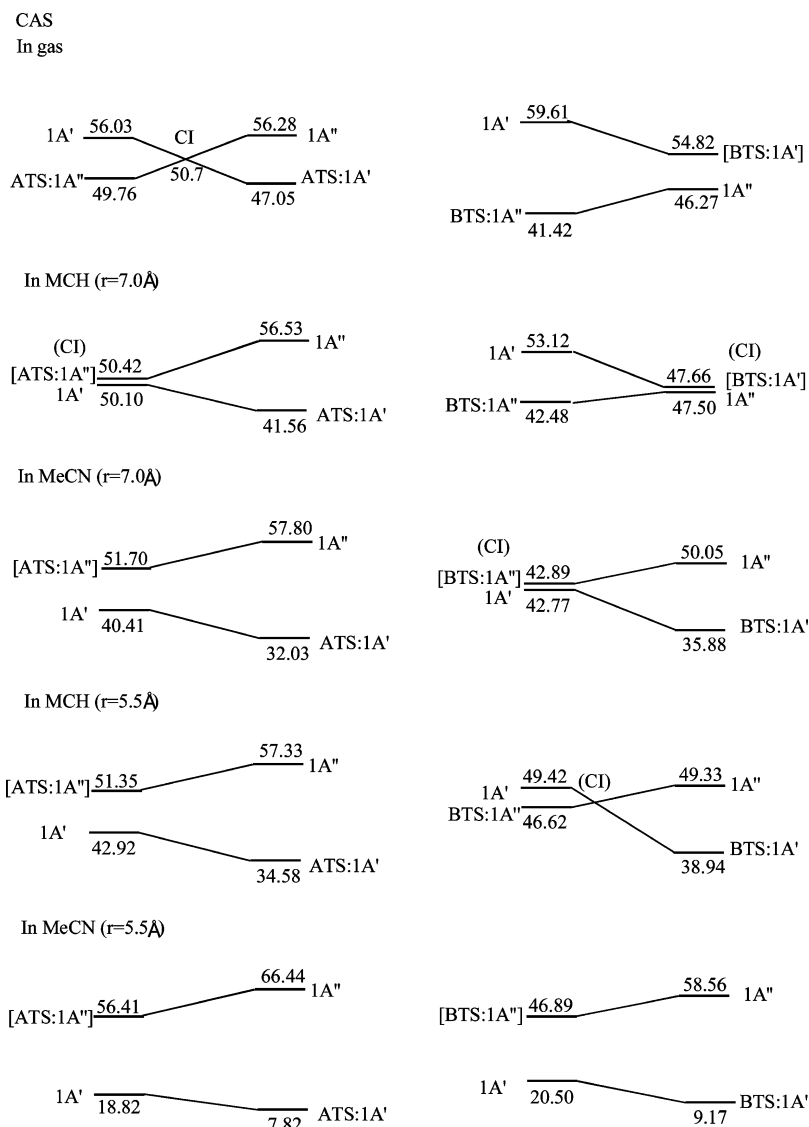


Figure 7. Relative CASSCF energies (kilocalories per mole) of the 1A' and 1A'' states at the optimized perpendicular transition structures (TS:1A' and TS:1A''). The left column is for the rotation around the b4 bond; the right column is for the rotation around the b6 bond.

which relates to isomerization around the b4 bond, using the MOLPRO program, which also allows the calculation of the energy gradient vector and the coupling vector. In this calculation, we had to use a smaller active space and a smaller basis set than that in the PC-GAMESS calculation. Starting with the PC-GAMESS result, the CI_A was located using MOLPRO and

optimized, and the g and h vectors were calculated. These data are presented in the Supporting Information. It is seen that the calculated structure of the CI_A is similar to that found by the PC-GAMESS calculation. The main difference is the somewhat shorter CN bonds. The g-h vectors fully agree with two coordinates of cis-trans isomerization loop, torsion and sym-

metric quinoidization distortion. Similar attempts to locate a conical intersection in the vicinity of the transition state of the b6 bond failed; the system did not converge to a CI. This result is also in line with the results of the PC-GAMESS calculation using the LH-loop method. (See Figures 6 and 7.) The MOLPRO calculation verifies the claim that in the gas phase, a photochemical isomerization through a conical intersection takes place around bond b4 and not around bond b6.

All three transition states located on the ground state in the gas phase have a relatively high barrier of over 40 kcal/mol at CASSCF level, impeding thermal isomerization at room temperature. However, upon optical excitation to the first $\pi \rightarrow \pi^*$ excited state, the promoted molecule can decay via the conical intersection CI_A to the two TS structures (ATS:1A' and ATS:1A'') on PES of the ground state, and the cis-trans photoisomerization around the b4 bond is expected to take place. Isomerization product A (Scheme 2) is obtained. As a result of the absence of a conical intersection for the rotation around the b6 double bond, the reaction forming product B is likely to be slower. Consequently, product A is predicted to be the preferred photochemical product in gas phase.

As Table 4 shows, the dipole moment of the ionic TS is much larger than that of the biradical TS. Therefore, in polar solvents, the ionic state (A') with larger dipole moment should be stabilized with respect to the biradical state (A''). It follows that in solvents, the photoisomerization products of MRCN might be different from those in the gas phase and could change upon varying polarity of solvent. Our calculations on reactions in the nonpolar MCH and the strongly polar MeCN solvents support this proposition.

Table 4 also indicates that the optimized ionic transition structure (TS:1A') in solution clearly has a lower barrier than that in the gas phase for both modes of isomerization. In contrast, the energy of biradical transition structure (TS:1A'') relative to the ground-state minimum hardly changes.

On the basis of the calculation with the larger cavity radius (7.0 Å), in MCH, the optimized biradical structure pertaining to the cis-trans isomerization around the b4 double bond lies on the excited-state potential surface because of the stabilization of the ionic state. At the optimized biradical structure, the energy of the lower ionic state (ground state) is almost equal to that of the biradical one (excited state), as shown in Figure 7. The energy gap between them is less than 1 kcal/mol, indicating that the optimized biradical structure for all practical purposes may be considered to be an efficient funnel, even if it is not formally a conical intersection. For the isomerization around the b6 double bond in MCH, although the ionic state of A' symmetry is higher in energy than the biradical state of A'' symmetry at both the optimized ionic and biradical perpendicular structures, the two electronic states (1A' and 1A'') are almost isoenergetic at the optimized ionic structure, so that the optimized ionic structure may practically act as an effective funnel. Therefore, in MCH, both isomerization products A and B are predicted to be formed with nearly equal probabilities upon irradiation. In the strongly polar solvent MeCN, because of the further stabilization of ionic state, no conical intersection exists for the cis-trans isomerization around the b4 double bond on the basis of the present CASSCF calculations. For the rotation of the b6 bond, the effective funnel from S_1 to S_0 has been moved to the optimized biradical structure. Therefore, in MeCN, product B is predicted to be the dominant photoisomerization product.

Calculations with a smaller radius (5.5 Å) predict a larger solvent effect on the ionic state. In MCH, only the conical

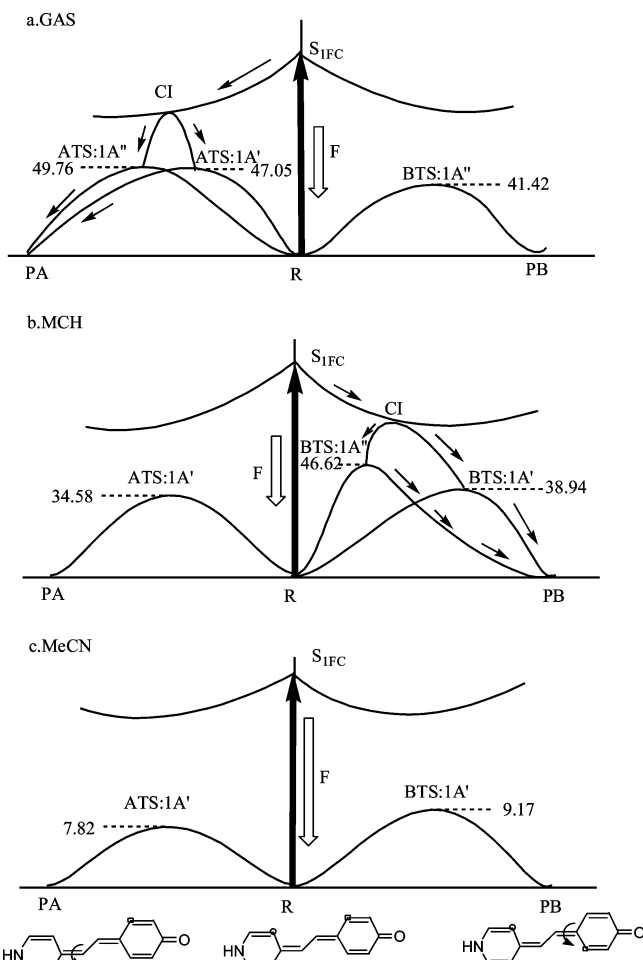


Figure 8. Schematic presentation of the solvent effect on the photoisomerization mechanism of MRCN. Because of the presence of a conical intersection (CI), product A is preferred in the gas phase, whereas in MCH, product B is preferred. In the polar solvent, the fluorescence yield (F) is enhanced because of the absence of a conical intersection, as indicated schematically by the length of the arrow.

intersection for the rotation around the b6 bond can be located between the two TS structures, suggesting product B as the preferred photoisomerization product. In MeCN, the barriers of both ionic TS states around the b4 and b6 bonds have been lower than 10 kcal/mol, similar to the rotation barrier (9.60 kcal/mol) of the central bond b5. In addition, a large energy gap (>1 eV) between the ionic state and biradical state is calculated for both of the rotations around b4 and b6 bonds. Therefore, the photoisomerization process is expected to notably slow down in polar solvents. The results obtained with the smaller cavity radius agree with some experimental observations: in polar solvents, the quantum yield of fluorescence is larger than that in nonpolar solvents.^{6a,61} Therefore, the solvent effect calculations using small radius appear to be in better agreement with experiments.

On the basis of the CASSCF results ($r = 5.5$ Å), in this work, the possible photoisomerization routes of MRCN in the gas phase and in solvents with different polarity are summarized in Figure 8.

In trying to correlate the above calculations with experiment, it is important to recall that on the basis of the present calculations, in the more polar solvent, all three CC bonds of the butadiene “bridge” appear to have the same length. The b5 bond in the ground state is a single bond in both the gas phase and nonpolar solvent; hence, the rotation of this bond is very

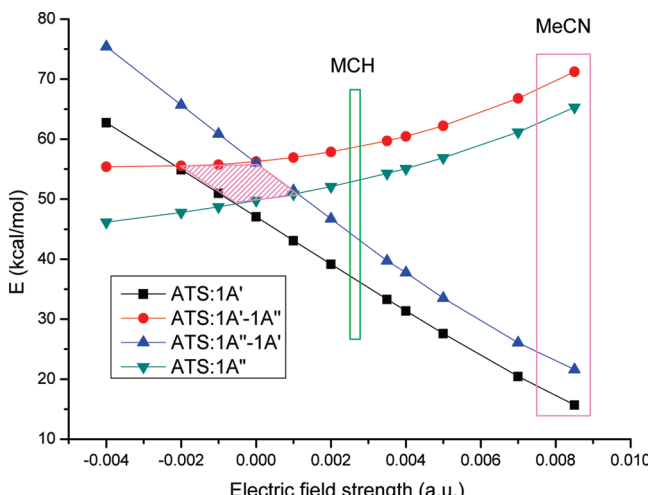


Figure 9. Barriers of the two optimized TS structures (ATS:1A' and ATS:1A'') for the rotation of the b4 bond and the relative energies of the 1A'' state at the ATS:1A' structure (ATS:1A'-1A'') and the 1A' state at the ATS:1A'' structure (ATS:1A''-1A'). The energy scale is relative to that of the ground-state equilibrium structure. In the hatched region, the conical intersection can be located.

facile having a very small energy barrier (3.18 kcal/mol in gas phase at the CASSCF level). In MeCN ($r = 5.5 \text{ \AA}$), the twisting barrier around the b5 bond is somewhat higher, 9.60 kcal/mol, comparable with the barriers for rotation around b4 (7.82) and b6 (9.17). It follows that all three possible reaction channels should be considered for this solvent. Anyway, the prediction is that a photoreaction, if triggered, is expected to be solvent-dependent.

III.3.B. Electric Field Effect on the Photoisomerization of MRCN. The calculations presented in Section III.1 show that applying an external electric field changes the relative weights of the two VB forms of the resonance hybrid of the ground-state of MRCN. The relative energies of the ionic and biradical states at perpendicular geometries could also be altered; therefore, the external electric field can be used to control the photoisomerization process, much like the solvent. Applying an external electric field may, in fact, be advantageous, because it can be continuously and smoothly modified and, in principle, is limited only by electric breakdown.

We have investigated the photoisomerization of MRCN by searching for the conical intersection between the two TS structures in the presence of an electric field (ef) varying from $\text{ef} = -0.004$ to 0.0085 au using CASSCF method. In the field range of $\text{ef} = -0.002$ to 0.001 au , a conical intersection is expected to be located in the hatched area shown in Figure 9 for the isomerization around the b4 bond. A CI or near crossing can probably also be found outside (but near to) this interval; the important photochemical consequence is that a rapid reaction is expected in the presence of these electric field strengths. Because the ionic perpendicular state for the isomerization around the b6 bond is on the first excited-state potential surface for this range, no conical intersection for this isomerization mode is anticipated to be found. Therefore, the photoisomerization product A is expected to be preferentially obtained in this range. In contrast, between $\text{ef} = 0.0015$ and 0.0035 au , a conical intersection for the isomerization around the b6 bond is expected to be located in the region of hatched area in Figure 10, whereas the conical intersection for the isomerization around the b4 bond disappears as a result of further stabilizing of the ionic state. The favored photoisomerization product of B is anticipated. In the range near 0.001 to 0.0015 au , both products A and B

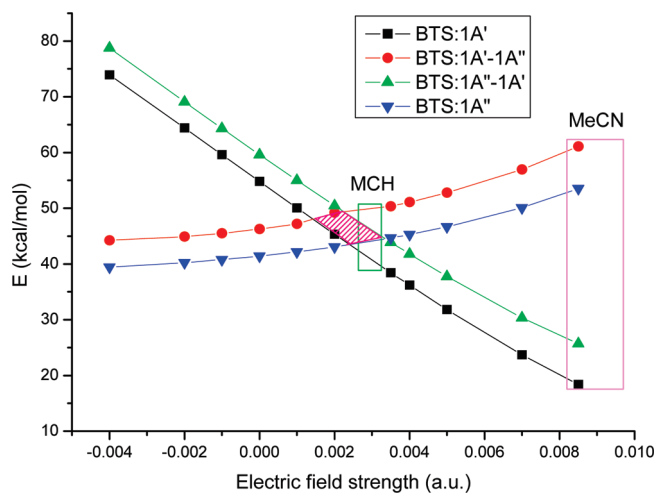


Figure 10. Barriers of the two optimized TS structures (BTS:1A' and BTS:1A'') for the rotation of the b6 bond and the relative energies of the 1A'' state at the BTS:1A' structure (BTS:1A'-1A'') and the 1A' state at the BTS:1A'' structure (BTS:1A''-1A'). The energy scale is relative to that of the ground-state equilibrium structure. In the hatched region, the conical intersection can be located.

are expected to coexist as a result of very small energy difference of the two states for both the rotations. The extent of the regioselectivity will be controlled by the interaction of charge effect and dynamics on the PES.²⁷

In practice, even when no conical intersection formally exists, the decay of S_1 to S_0 can be very rapid if the energy gap between them is small. A gap smaller than 0.5 to 1 eV is believed to be small enough to ensure rapid internal conversion. Therefore, both products A and B can be observed experimentally in a large range between -0.002 and 0.004 au . For electric fields larger than 0.005 au , the energy gap of the two PESs for the rotation of the b4 bond becomes large enough ($>1 \text{ eV}$) to favor product B strongly. In the same way, if the antiparallel electric field is stronger than 0.0027 au , then product A becomes the favorable product.

Comparing the CASSCF calculations in solvents and in the presence of electric fields, one finds that the effect of MCH ($r = 5.5 \text{ \AA}$) is similar to electric fields in the 0.0025 to 0.0032 au range, and MeCN ($r = 5.5 \text{ \AA}$) acts like fields in the 0.0074 to 0.0096 au range. The energy of the biradical state of the isomerization around the b6 bond is lower than that of the isomerization around the b4 bond under all field strengths; in contrast, the ionic state lies at a higher energy than that pertaining to the isomerization around the b4 bond. Therefore, when the ionic state that is on the excited state PES is stabilized by degrees under the application of increasing electric field, the conical intersection connecting the ionic and biradical states of the isomerization around the b4 bond appears before that of the isomerization around the b6 bond and also disappears at lower fields. Therefore, it may be possible, in principle, to tune the isomerization product (A or B) of MRCN by controlling the surrounding environment under the irradiation. The MRCN molecule may thus be a good candidate for a molecular switch.

IV. Summary

This article presents a three-state model advanced to account for the photochemistry of MRCN. CASSCF calculations serve to provide numerical estimates for the important three electronic states involved in the process in two parts of the potential surface: the Franck-Condon region and the vicinity of the conical intersection. The main novel result is the strong effect

that solvents and static electric fields have on the energy structure of the molecule in these regions. This is related to the fact that the ground state wave function may be considered to be the in-phase combination of two main VB wave functions: quinonoid and a zwitterion. In the gas phase, the quinonoid VB form is predominating in the resonance hybrid of the ground state ($c^2 = 0.32$, eq 1). The weight of the zwitterion structure in the ground state increases upon the increasing the polarity of the solvent or upon the increasing strength of an external electric field augmenting the molecular dipole. At a field of 0.01 au, c^2 becomes 0.53, and the molecule is in the cyanine limit. At still higher electric fields, the ground-state structure can be transformed to a pure zwitterion structure.

Comparing our calculations with experimental observations, the CASSCF method appears to overestimate slightly the weight of the quinonoid structure in the resonance hybrid; whereas, the DFT-B3LYP method seems to underestimate it.

In addition to the ground state, two excited states are considered: a twin state of the ground state formed by the out-of-phase combination of the quinonoid and zwitterion VB forms and a biradical state, which are the two lowest-lying excited states of MRCN.

In the isolated molecule, the biradical state is the first $\pi \rightarrow \pi^*$ excited state in the Franck–Condon region, but upon applying an external electric field, the energy of the twin state is lowered, and the twin state definitely becomes S₁.

The photoisomerization of MRCN can occur around bonds b4 and b6, leading to two different products; this case is similar to that demonstrated experimentally in ref 27. Conical intersections were calculated for both reaction modes under different conditions. The present calculations suggest that in the region of the field strength varying from -0.002 to 0.004 au, both photoisomerization products A and B can be observed experimentally. In the presence of an electric field strength of ~ 0.005 au (or ~ -0.0027 au), product B predominates (or A). In stronger fields, photoisomerization is less efficient. Calculations using an Onsager model (cavity radius = 5.5 Å) show that the effect of the nonpolar solvent MCH is similar to that of $\epsilon_f = 0.0025$ to 0.0032 au, whereas the highly polar MeCN acts as an electric field between 0.0074 and 0.0096 au. Therefore, in MCH, the existence of a conical intersection promotes photoisomerization, leading to weak fluorescence of the excited MRCN, whereas in MeCN, the photoisomerization reaction is slower, resulting in higher fluorescence efficiency in MeCN than that in MCH, as observed experimentally. In highly polar solvents such as MeCN and in the presence of strong electric fields, the twisting barrier around the b5 bond is comparable to the barriers for rotation around b4 and b6. All three possible reaction channels should be considered for this solvent. In any case, our calculations predict that a photoreaction, if triggered, is expected to be solvent-dependent.

It is shown that the photoisomerization products of MRCN can be switched through adjusting the environment. Therefore, the MRCN molecule can be a candidate of the molecular switches.

Acknowledgment. Financial support from the DFG within the trilateral project Germany–Israel–Palestine Ma-515/22-2 is gratefully acknowledged. A.K. thanks the Ministry of Science and Technology for a Levy Eshkol Scholarship. We acknowledge with deep appreciation collaboration with Prof. J. Manz, Prof. L. Gonzales, Dr. M. Leibscher, and Prof. O. Deeb; discussions with all of them contributed significantly to the ideas developed in this work. We also thank Prof. T. Seideman for

many enlightening discussions. The Minerva Farkas Center for Light Induced Processes is supported by the Minerva Gesellschaft mbH.

Supporting Information Available: Frontier molecular orbitals, natural orbitals involved in the active space, CASSCF obtained geometries of transition states (TS:1A', TS:1A'') and conical intersection (CI) in different solvents, Mulliken charge distributions of the ground-state minimum and the transition structures for both of the rotations around b4 and b6 bonds, relative CAS energies of the 1A' and 1A'' states at the optimized transition structures, results of the CI calculation, main bond lengths for the optimized ground-state minima, calculated dipole moments and BLA parameters for the optimized ground-state equilibrium geometries, main bond length for the optimized ground-state minima, relative energy and dipole moment of the optimized transition states in electric fields, imaginary frequency of the optimized perpendicular transition structures, and calculated gradient difference and derivative coupling of CI_A. This material is available free of charge via the Internet at <http://pubs.acs.org>.

References and Notes

- Brooker, L. G. S.; Keyes, G. H.; Sprague, R. H.; van Dyke, R. H.; van Lare, E.; van Zandt, G.; White, F. L. *J. Am. Chem. Soc.* **1951**, *73*, 5326.
- Jacques, P. *J. Phys. Chem.* **1986**, *90*, 5535.
- Brooker, L. G. S.; Craig, A. C.; Heseltine, D. W.; Jenkins, P. W.; Lincoln, L. L. *J. Am. Chem. Soc.* **1965**, *87*, 2443.
- Reichardt, C. *Solvents and Solvent Effects in Organic Chemistry*; Verlag Chemie: New York, 1988 and references therein.
- Morley, J. O.; Morley, R. M.; Fitton, A. L. *J. Am. Chem. Soc.* **1998**, *120*, 11479.
- (a) Baraldi, I.; Brancolini, G.; Momicchioli, F.; Ponterini, G.; Vanossi, D. *Chem. Phys.* **2003**, *288*, 309. (b) Rettig, W.; Dekhtyar, M. *Chem. Phys.* **2003**, *293*, 75, and references therein.
- Guillaume, M.; Champagne, B.; Zutterman, F. *J. Phys. Chem. A* **2006**, *110*, 13007.
- Steiner, U.; Abdel-Kader, M. H.; Fisher, P.; Kramer, H. E. A. *J. Am. Chem. Soc.* **1978**, *100*, 3190.
- Tavan, P.; Schulten, K. *Chem. Phys. Lett.* **1984**, *110*, 191.
- Gaines, G. L. *Angew. Chem., Int. Ed. Engl.* **1987**, *26*, 341.
- Burda, C.; Abdel-Kader, M. H.; Link, S.; El-Sayed, M. A. *J. Am. Chem. Soc.* **2000**, *122*, 6720.
- Gómez, I.; Reguero, M.; Robb, M. A. *J. Phys. Chem. A* **2006**, *110*, 3986.
- Mandal, D.; Pal, S. K.; Sukul, D.; Bhattacharyya, K. *J. Phys. Chem. A* **1999**, *103*, 8156.
- Baraldi, I.; Momicchioli, F.; Ponterini, G.; Tatikolov, A. S.; Vanossi, D. *Phys. Chem. Chem. Phys.* **2003**, *5*, 979.
- Marder, S. R.; Gorman, C. B.; Meyers, F.; Perry, J. W.; Bourhill, G.; Bredas, J.-L.; Pierce, B. M. *Science* **1994**, *265*, 632.
- Bosshard, C.; Pan, F.; Wong, M. S.; Manetta, S.; Spreiter, R.; Cai, C.; Günter, P.; Gramlich, V. *Chem. Phys.* **1999**, *245*, 377.
- Sainudeen, Z.; Ray, P. C. *J. Phys. Chem. A* **2005**, *109*, 9095.
- Ray, P. C.; Bonifassi, P.; Leszczynski, J. *J. Phys. Chem. A* **2006**, *110*, 8963.
- Mineo, Y.; Itoh, K. *J. Phys. Chem.* **1991**, *95*, 2451.
- Lambert, C.; Stadler, S.; Bourhill, G.; Bräuchle, C. *Angew. Chem., Int. Ed. Engl.* **1996**, *35*, 644.
- Abbotto, A.; Beverina, L.; Bradamante, S.; Facchetti, A.; Klein, C.; Pagani, G. A.; Redi-Abshire, M.; Wortmann, R. *Chem.—Eur. J.* **2003**, *9*, 1991.
- Ray, P. C. *Chem. Phys. Lett.* **2004**, *395*, 269.
- Pan, F.; Wong, M. S.; Gramlich, V.; Bosshard, C.; Günter, P. *J. Am. Chem. Soc.* **1996**, *118*, 6315.
- Albert, I. D. A.; Marks, T. J.; Ratner, M. A. *J. Phys. Chem.* **1996**, *100*, 9714.
- Zilberg, S.; Haas, Y. *J. Phys. Chem. A* **1998**, *102*, 10843.
- Würthner, F.; Archetti, G.; Schmidt, R.; Kuball, H.-G. *Angew. Chem., Int. Ed. Engl.* **2008**, *47*, 4529.
- Squillacote, M.; Wang, J.; Chen, J. *J. Am. Chem. Soc.* **2004**, *126*, 1940.
- Haas, Y.; Cogan, S.; Zilberg, S. *Int. J. Quantum Chem.* **2005**, *102*, 961.
- Zilberg, S.; Haas, Y. *Photochem. Photobiol. Sci.* **2003**, *2*, 1256.

- (30) Haas, Y.; Cogan, S.; Kahan, A.; Zilberg, S. *J. Phys. Chem. A* **2008**, *112*, 5604.
- (31) Herzberg, G.; Longuet-Higgins, H. C. *Discuss. Faraday Soc.* **1963**, *35*, 77.
- (32) Longuet-Higgins, H. C. *Proc. R. Soc. London, Ser. A* **1975**, *344*, 147.
- (33) Zilberg, S.; Haas, Y. *Chem.—Eur. J.* **1999**, *5*, 1755.
- (34) Jasper, A. W.; Kendrick, B. K.; Mead, C. A.; Truhlar, D. G. In *Modern Trends in Chemical Reaction Dynamics*; Yang, X., Liu, K., Eds.; Advanced Series in Physical Chemistry 14; Word Scientific: River Edge, NJ, 2004; pp 329–391.
- (35) Tishchenko, O.; Truhlar, D. G.; Ceulemans, A.; Nguyen, M. T. *J. Am. Chem. Soc.* **2008**, *130*, 7000.
- (36) (a) Roos, B. O. *Adv. Chem. Phys.* **1987**, *69*, 399. (b) Roos, B. O. In *Ab Initio Methods in Quantum Chemistry II*; Lawley, K. P., Ed.; Wiley: New York, 1987; p 399. (c) Werner, H.-J.; Knowles, P. J. *J. Chem. Phys.* **1985**, *82*, 5053. (d) Knowles, P. J.; Werner, H.-J. *Chem. Phys. Lett.* **1985**, *115*, 259. (e) Busch, T.; Degli Esposti, A.; Werner, H.-J. *J. Chem. Phys.* **1991**, *94*, 6708.
- (37) Granovsky, A. A. *PC GAMESS*, version 7.0. <http://classic.chem.msu.su/gran/games/index.html>.
- (38) Werner, H.-J.; Knowles, P. J.; Amos, R. D.; Bernhardsson, A.; Berning, A.; Celani, P.; Cooper, D. L.; Deegan, M. J. O.; Dobbyn, A. J.; Eckert, F.; Hampel, C.; Hetzer, G.; Korona, T.; Lindh, R.; Lloyd, A. W.; McNicholas, S. J.; Manby, F. R.; Meyer, W.; Mura, M. E.; Nicklass, A.; Palmieri, P.; Pitzer, R.; Rauhut, G.; Schütz, M.; Schumann, U.; Stoll, H.; Stone, A. J.; Tarroni, R.; Thorsteinsson, T. *MOLPRO, A Package of Ab Initio Programs*, version 2002.1; University of Birmingham: Birmingham, U.K., 2001.
- (39) The only large scale computation on a merocyanine reported so far is by Robb, J. *Phys. Chem. A* **2006**, *110*, 3986, in which a smaller molecule was considered and the reaction was a ring closure one (merocyanine to spiropyran).
- (40) Boggio-Pasqua, M.; Bearpark, M. J.; Klene, M.; Robb, M. A. *J. Chem. Phys.* **2004**, *120*, 7849.
- (41) Dallos, M.; Lischka, H. *Theor. Chem. Acc.* **2004**, *112*, 16.
- (42) Blomgren, F.; Larsson, S. *Int. J. Quantum Chem.* **2002**, *90*, 1536.
- (43) Bachler, V. *J. Comput. Chem.* **2003**, *25*, 343.
- (44) Ostojic, B.; Domcke, W. *Chem. Phys.* **2001**, *269*, 1.
- (45) Serrano-Andrés, L.; Roos, B. O.; Merchán, M. *Theor. Chim. Acta* **1994**, *87*, 387.
- (46) Serrano-Andrés, L.; Merchán, M.; Nebot-Gil, I.; Lindh, R.; Roos, B. O. *J. Chem. Phys.* **1993**, *98*, 3151.
- (47) Schmidt, M. W.; Baldridge, K. K.; Boatz, J. A.; Elbert, S. T.; Gordon, M. S.; Jensen, J. H.; Koseki, S.; Matsunaga, N.; Nguyen, K. A.; Su, S.; Windus, T. L.; Dupuis, M.; Montgomery, J. A., Jr. *J. Comput. Chem.* **1993**, *14*, 1347.
- (48) Dick, B. *J. Chem. Theory Comput.* **2009**, *5*, 116. See also: Dick, B.; Haas, Y.; Zilberg, S. *Chem. Phys.* **2008**, *347*, 65.
- (49) (a) Kirkwood, J. *J. Chem. Phys.* **1934**, *2*, 351. (b) Onsager, L. *J. Am. Chem. Soc.* **1936**, *58*, 1486.
- (50) Becke, A. D. *J. Chem. Phys.* **1993**, *98*, 5648.
- (51) Lee, C.; Yang, W.; Parr, R. G. *Phys. Rev.* **1988**, *B37*, 785.
- (52) Frisch, M. J.; Trucks, G. W.; Schlegel, H. B.; Scuseria, G. E.; Robb, M. A.; Cheeseman, J. R.; Zakrzewski, V. G.; Montgomery, J. A., Jr.; Stratmann, R. E.; Burant, J. C.; Dapprich, S.; Millam, J. M.; Daniels, A. D.; Kudin, K. N.; Strain, M. C.; Farkas, O.; Tomasi, J.; Barone, V.; Cossi, M.; Cammi, R.; Mennucci, B.; Pomelli, C.; Adamo, C.; Clifford, S.; Ochterski, J.; Petersson, G. A.; Ayala, P. Y.; Cui, Q.; Morokuma, K.; Malick, D. K.; Rabuck, A. D.; Raghavachari, K.; Foresman, J. B.; Cioslowski, J.; Ortiz, J. V.; Stefanov, B. B.; Liu, G.; Liashenko, A.; Piskorz, P.; Komaromi, I.; Gomperts, R.; Martin, R. L.; Fox, D. J.; Keith, T.; Al-Laham, M. A.; Peng, C. Y.; Nanavakkara, A.; Gonzalez, C.; Challacombe, M.; Gill, P. M. W.; Johnson, B.; Chen, W.; Wong, M. W.; Andres, J. L.; Gonzalez, C.; Head-Gordon, M.; Replogle, E. S.; Pople, J. A. *Gaussian 03*, revision B.03; Gaussian, Inc.: Pittsburgh, PA, 2003.
- (53) Miertus, S.; Scrocco, E.; Tomasi, J. *Chem. Phys.* **1981**, *55*, 117.
- (54) Willetts, A.; Rice, J. E. *J. Chem. Phys.* **1993**, *99*, 426.
- (55) All comparisons with experiments were done with data obtained for Brooker's merocyanine rather than I.
- (56) Baumann, W. Z. *Naturforscher* **1983**, *38a*, 995.
- (57) Bletz, M.; Pfeifer-Fukumura, U.; Kolb, U.; Baumann, W. *J. Phys. Chem. A* **2002**, *106*, 2232.
- (58) Meyers, F.; Marder, S. R.; Pierce, B. M.; Brédas, J. L. *J. Am. Chem. Soc.* **1994**, *116*, 10703, and ref 25 therein.
- (59) The Cs restriction simulates the experimental situation in a solid matrix, in which torsion is inhibited, as outlined in the Introduction.
- (60) Fuss, W.; Haas, Y.; Zilberg, S. *Chem. Phys.* **2000**, *259*, 273.
- (61) Ischenko, A. A.; Kulinich, A. V.; Bondarev, S. L.; Knyuksho, V. N. *J. Phys. Chem. A* **2007**, *111*, 13629.

JP904097K